3-31-2014

Transition to Order After Hilltop Inflation

Marcelo Gleiser
Dartmouth College

Noah Graham
Middlebury College

Transition To Order After Hilltop Inflation

Marcelo Gleiser[1,*] and Noah Graham[2,†]

[1] *Center for Cosmic Origins and Department of Physics and Astronomy Dartmouth College, Hanover, NH 03755, USA*

[2] *Department of Physics, Middlebury College, Middlebury, VT 05753, USA*

We investigate the rich nonlinear dynamics during the end of hilltop inflation by numerically solving the coupled Klein-Gordon-Friedmann equations in a expanding universe. In particular, we search for coherent, nonperturbative configurations that may emerge due to the combination of nontrivial couplings between the fields and resonant effects from the cosmological expansion. We couple a massless field to the inflaton to investigate its effect on the existence and stability of coherent configurations and the effective equation of state at reheating. For parameters consistent with data from the Planck and WMAP satellites, and for a wide range of couplings between the inflaton and the massless field, we identify a transition from disorder to order characterized by emergent oscillon-like configurations. We verify that these configurations can contribute a maximum of roughly 30% of the energy density in the universe. At late times their contribution to the energy density drops to about 3%, but they remain long-lived on cosmological time-scales, being stable throughout our simulations. Cosmological oscillon emergence is described using a new measure of order in field theory known as relative configurational entropy.

PACS numbers: 98.80Cq,11.10.Lm, 11.15.Ex

I. INTRODUCTION

Recent results from the Planck satellite have placed severe constraints on viable models of inflation [1]. Quoting from Ref. [2], "Constraints on inflationary models are presented in Planck Collaboration XXII [1] and overwhelmingly favor a single, weakly coupled, neutral scalar field driving the accelerated expansion and generating curvature perturbations." In addition, exponential potentials, the simplest hybrid inflation models, and monomial potential models with $n \geq 2$ do not provide a good fit to the data [1, 3]. Models with non-minimal gravitational coupling are less constrained, but we will focus here on ordinary gravity. Combined data from the Planck satellite, from the WMAP satellite [4], and from measurements of the baryon acoustic oscillations (BAO) scale [5] favor models with $V'' < 0$, in particular hilltop models such as the original new inflation scenario of Albrecht and Steinhardt [6] and Linde [7] based on a Coleman-Weinberg (CW) potential. If such models are considered near the origin ($\phi \gtrsim 0$), they can be approximated as

$$V(\phi) \simeq \Lambda^4 \left(1 - \frac{\phi^p}{\mu^p}\right), \tag{1}$$

where p is a positive integer. Here $p = 2$ is allowed only as a large-field model, while $p = 3$ lies outside the 95% confidence level (CL) for Planck+WMAP+BAO. However, $p = 4$, the model we are interested in, is allowed within the joint 95% CL for a number of e-folds $N_* = \int_{t_*}^{t_e} dt H \gtrsim 50$. The * means that the number of e-folds is computed when the mode $k_* = a_* H_* = 0.002(8\pi G)^{1/2}$ (the pivot scale) crosses the Hubble radius for the first time [8, 9]. Models with higher values of p are within the accepted range, but are less well-motivated from high-energy physics. Taking these constraints together, it is important to investigate the late-time dynamics of CW new inflation style potentials, in particular in regards to the possible emergence of nonperturbative coherent structures during the preheating phase of inflation [10–12]. This is when the inflaton performs near-linear oscillations about the potential minimum, and the universe begins to transition to a power-law expansion, during which time entropy is generated profusely to produce the hot Big Bang. We should note that there are other models consistent with the combined data, such as natural inflation [13, 14], but in the late-time regime that we are considering they will behave similarly to CW models.

Given the nonlinear nature of the reheating dynamics, it is natural to investigate whether extended coherent structures may be formed as the oscillating inflaton gives up its energy to different modes and, potentially, to other

*Electronic address: mgleiser@dartmouth.edu

†Electronic address: ngraham@middlebury.edu

fields. Clearly, such processes will play a decisive role in the reheating process and the transition to a power-law expansion. Indeed, much recent work has been devoted to answering this question in a variety of inflationary models. If we focus only on real scalar field models, the dominant coherent configurations are oscillons [15–17]: long-lived, time-dependent localized configurations which have been shown to exist in many models of interest in cosmology and high-energy physics, from Abelian Higgs models [18, 19] to the Standard Model (for particular parameter values) [20–22]. Within inflation, inflaton "hot spots" were reported in Ref. [23], while "condensate lumps" were found for a class of supersymmetric models in Ref. [24]. The potential role of oscillons in cosmology has been investigated in 1d simulations [25–28], while 3d simulations have been carried out for a single real field in a double-well potential [29], for hybrid inflation [30], and for ϕ^6 potentials [31], where the emergence of flat-top oscillons [28] was reported. Formation of oscillons after inflation for realistic inflationary potentials was investigated in [32], which prompted one of the questions we address here: whether couplings to other fields destabilize oscillons over time scales shorter than those associated with quantum mechanical decays [33]. As will be shown here, they do not, at least for the class of models we investigated. If oscillons are sufficiently long-lived, that is, if their lifetime is at least of order of H^{-1}, and if they contribute significantly to the energy density, they can have important cosmological consequences: for example, delaying thermalization and thus lowering the thermalization temperature [34]; changing the effective potential and seeding spontaneous symmetry breaking [35]; and, if they decay, producing entropy, and possibly generating gravitational waves [36].

This paper is organized as follows. In the next section we introduce the model and describe the details of the numerical simulations. In Section 3 we describe our results, using two measures to account for the emergence of oscillons: their fractional contribution to the energy density, and, for the first time in cosmology, the more precise relative configurational entropy [37, 38]. As we shall see, oscillons emerge for a wide range of model parameters consistent with the Planck+WMAP+BAO data and contribute a nontrivial fraction of the energy density. Furthermore, we show that they remain stable over cosmological time-scales. We conclude in Section 4 with a summary of our results.

II. COLEMAN-WEINBERG INFLATION

We consider a model of slow-roll inflation with a Coleman-Weinberg potential for the real scalar inflaton field ϕ, which is also coupled quadratically to a massless real scalar χ. The Lagrangian density in comoving coordinates is

$$\mathcal{L} = \frac{1}{2}\int a(t)^3 \left[(\partial_\mu\phi)(\partial^\mu\phi) + (\partial_\mu\chi)(\partial^\mu\chi) - \frac{\lambda}{4}\left(\phi^4\log\frac{\phi^2}{\nu^2} + \frac{1}{2}\nu^4 - \frac{1}{2}\phi^4\right) - h^2\phi^2\chi^2\right] d^3x\,, \tag{2}$$

where h is the coupling to the light field χ, which will allow for decay of the inflaton at reheating, and $a(t)$ is the expansion factor from the usual Robertson-Walker metric [39]. The coupling λ can be thought of as coming from self-interactions of the field ϕ and/or from summing over one-loop corrections from gauge bosons and/or fermions. (In the original model new inflation model, those bosons were thought to come from an $SU(5)$ GUT [6, 7].) From the Lagrangian density, we obtain the equations of motion for the two fields as

$$\ddot{\phi} + 3H\dot{\phi} - \frac{\nabla^2\phi}{a(t)^2} = -\frac{1}{2}\lambda\phi^3\log\left(\frac{\phi^2}{\nu^2}\right) - h^2\chi^2\phi \tag{3}$$

$$\ddot{\chi} + 3H\dot{\chi} - \frac{\nabla^2\chi}{a(t)^2} = -h^2\phi^2\chi, \tag{4}$$

where we have written the Hubble parameter as $H = \frac{\dot{a}(t)}{a(t)}$. The evolution of the scale factor $a(t)$ is given by the Friedmann equation

$$H^2 = \frac{1}{3m_{\rm pl}^2}\left[\frac{1}{2}\dot{\phi}^2 + \frac{1}{2}\dot{\chi}^2 + \frac{1}{2}\frac{(\nabla\phi)^2}{a^2} + \frac{1}{2}\frac{(\nabla\chi)^2}{a^2} + \frac{\lambda}{8}\left(\phi^4\log\frac{\phi^2}{\nu^2} + \frac{1}{2}\nu^4 - \frac{1}{2}\phi^4\right) + \frac{1}{2}h^2\phi^2\chi^2\right], \tag{5}$$

where $m_{\rm pl} \equiv (8\pi G)^{-1/2}$ is the reduced Planck mass. The inflaton will slow-roll until it reaches its inflection point. During slow-roll, the expansion is well-approximated by a pure de Sitter metric. After the inflection point, ϕ will perform large-amplitude oscillations about the minimum at ν. These oscillations, due to the self-coupling of ϕ, will be responsible for generating oscillons through parametric amplification. This mechanism has been discussed in detail in Refs. [29], [30], and [31]. After very long times, the oscillations damp away, leaving the field ϕ at its vacuum expectation value ν, where it has a mass $m_\phi = \nu\sqrt{\lambda}$ and gives mass $m_\chi = h\nu$ to the χ particle. For oscillons to form,

ν cannot be too close to the Planck mass, because in that case the characteristic oscillon size is comparable to the Hubble length and the expansion of the universe prevents their formation [29]. In our simulations we take $m_{\rm pl} = 100\nu$, and so $\nu \simeq 2.43 \times 10^{16}\,{\rm GeV}$.

In order to produce density fluctuations compatible with those observed in the cosmic microwave background, we choose a very small self-coupling, $\lambda = 1.5 \times 10^{-13}$. We begin our simulations when the slow-roll process starting from $\phi \approx 0$ has reached $\phi_{\rm inf}/2$, halfway to the inflection point at $\phi_{\rm inf} = \nu e^{-1/3} \simeq 1.74 \times 10^{16}\,{\rm GeV}$ that signals the end of inflation. To set the initial conditions for our simulation, we add zero-point fluctuations to this classical value of ϕ and also include zero-point fluctuations in the χ field. Our initial state is thus given solely by zero-point fluctuations about a classical value: there are no coherent field configurations present. In this sense we call it a disordered state.

The simulation space consists of a cube with comoving size L and volume $V = L^3$ discretized on a regular lattice with spacing $\Delta x^i = \Delta r$ $(i = 1, 2, 3)$. We simulate the initial conditions for each field as quantum perturbations around their homogeneous values $\phi = \phi_{\rm inf}/2 = \nu e^{-1/3}/2$ and $\chi = 0$. We use periodic boundary conditions. To set up the initial conditions, we label both free fields' normal modes by $\mathbf{k} = (2\pi \mathbf{n}_i/L)$, where $\mathbf{n} = (n_x, n_y, n_z)$ and the n_i are integers $n_i = -N/2+1 \ldots N/2$. Here $N = L/\Delta r$ is the number of lattice points per side. Each free mode is described by a harmonic oscillator with frequency $\omega_k^2 = (2\sin(k\Delta r/2)/\Delta r)^2 + m_{\rm eff}^2$, where $k = |\mathbf{k}|$ and $m_{\rm eff}$ is the effective mass of each field given above. The initial conditions for the fields are then given by [30]

$$\begin{aligned} \phi(\mathbf{r}, t=0) &= \frac{\phi_{\rm inf}}{2} + \frac{1}{\sqrt{V}} \sum_{\mathbf{k}} \sqrt{\frac{1}{2\omega_k}} \left[\alpha_k e^{i\mathbf{k}\cdot\mathbf{r}} + \alpha_k^* e^{-i\mathbf{k}\cdot\mathbf{r}}\right], \\ \dot{\phi}(\mathbf{r}, t=0) &= \frac{1}{\sqrt{V}} \sum_{\mathbf{k}} \frac{1}{i} \sqrt{\frac{\omega_k}{2}} \left[\alpha_k e^{i\mathbf{k}\cdot\mathbf{r}} - \alpha_k^* e^{-i\mathbf{k}\cdot\mathbf{r}}\right], \end{aligned} \tag{6}$$

$$\begin{aligned} \chi(\mathbf{r}, t=0) &= \frac{1}{\sqrt{V}} \sum_{\mathbf{k}} \sqrt{\frac{1}{2\omega_k}} \left[\alpha_k e^{i\mathbf{k}\cdot\mathbf{r}} + \alpha_k^* e^{-i\mathbf{k}\cdot\mathbf{r}}\right], \\ \dot{\chi}(\mathbf{r}, t=0) &= \frac{1}{\sqrt{V}} \sum_{\mathbf{k}} \frac{1}{i} \sqrt{\frac{\omega_k}{2}} \left[\alpha_k e^{i\mathbf{k}\cdot\mathbf{r}} - \alpha_k^* e^{-i\mathbf{k}\cdot\mathbf{r}}\right], \end{aligned} \tag{7}$$

where α_k is a random complex variable with phase distributed uniformly on $[0, 2\pi)$ and magnitude drawn from a Gaussian distribution such that $\langle |\alpha_k|^2 \rangle = 1/2$.

The evolution of the expansion rate in dimensionless units is given by solving Eqs. (3) and (4) together with the volume-averaged Friedmann equation

$$H^2 = \frac{1}{3} \frac{\langle \rho \rangle}{m_{\rm pl}^2}, \tag{8}$$

where $\langle \rho \rangle$ is the volume-averaged energy density. At each time step, we solve the coupled equations for ϕ and χ, and for the scale factor $a(t)$, using $H = \dot{a}(t)/a(t)$ and $a(t=0) = 1$. We discretize the equations with initial spacing $\delta = 1/(32 m_\phi)$ and size $16/m_\phi$, yielding a box with 512^3 lattice points. We keep the same lattice in comoving coordinates, and solve the field theory equations of motion in the presence of the expanding scale factor $a(t)$. When seeding the initial lattice, we only excite modes up to wave number $k = 1/(2\delta)$ to avoid limitations of the numerical calculation near the Nyquist frequency. We performed very long runs, out to scale factors $a(t_{\rm end}) \approx 10$, which corresponds to total time $t_{\rm end} \approx 15,000/m_\phi$. With a slower expansion rate, these runs are considerably longer than those in our previous analysis of oscillon formation in hybrid inflation [30]. Longer runs, while clearly more CPU-intensive, allow us to investigate more fully the long-time behavior of oscillons, in particular their longevity. Indeed, we found that in models that allow for the formation of oscillons, their long-term contribution amounts to approximately 3% of the total energy density and remains stable at late times.

III. EMERGENT STRUCTURES DURING PREHEATING

A. Equation of State

We first plot the spatially-averaged values of the ϕ and χ fields in Fig. 1 for different values of the coupling h. The vertical dashed line (red online) marks the time after which oscillations of the inflaton can no longer climb above the inflection point. (That is, from then on $\phi > \phi_{\rm inf}$.) The initial oscillations of the ϕ field as it reaches its vev induce

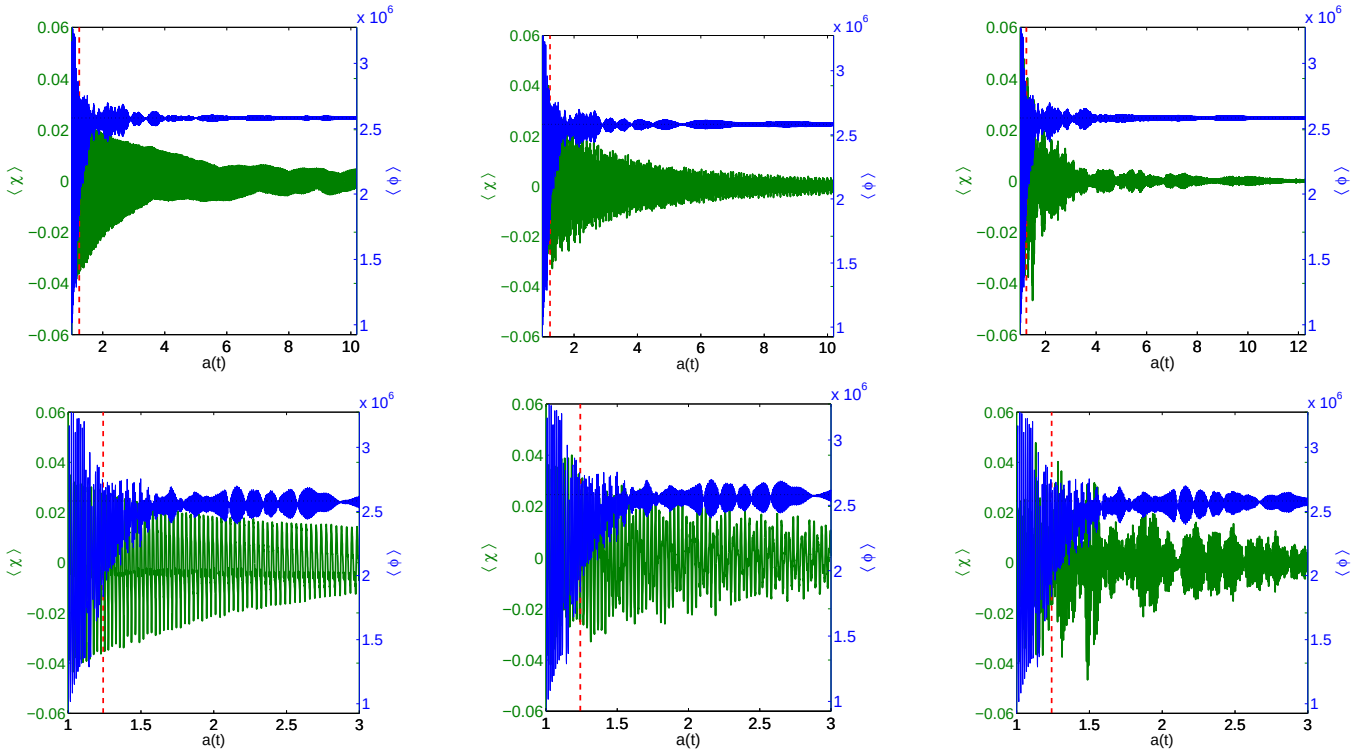

FIG. 1: (Color online.) Volume-averaged values of ϕ and χ as functions of the expansion factor $a(t)$, in units of m_ϕ. Results are shown for $\lambda = 1.5 \times 10^{-13}$, $m_{\rm pl} = 100\nu$, and $h = \sqrt{\lambda}/100$ (left), $h = \sqrt{\lambda}/10$ (center), and $h = \sqrt{\lambda}$ (right). The top row shows the entire run, while the bottom row zooms in on the initial period when oscillons are forming. The vertical dashed line indicates the time when oscillations of the inflaton can no longer reach the inflection point.

oscillations of the χ field through parametric resonance. During this process, localized oscillations in the ϕ field emerge, which then form into oscillons, as we will see below. In Fig. 2 we show the evolution of the spatially-averaged fields when their mutual coupling is zero ($h = 0$). We can see that when $h \neq 0$ the initial energy of the inflaton is rapidly transferred to the χ field and that nonlinear effects for the χ field become more pronounced as h increases. In contrast, the behavior of the inflaton is quite similar for all cases when $h \neq 0$. This is reflected in the production of oscillons, as we will see below. When $h = 0$ there is no energy transfer between the two fields and the χ field remains essentially at its initial value, except for quantum fluctuations. We note the sharp change in the behavior of the inflaton in this case: as it drops beyond its inflection point, the amplitude of oscillations is rapidly suppressed. Contrasting with the case when $h \neq 0$, we see that the coupling with the χ field sustains larger-amplitude oscillations of the inflaton for longer times, generating a richer nonlinear dynamics.

Next we track the equation of state by computing the ratio $w = \langle p\rangle/\langle\rho\rangle$, where $\langle p\rangle$ is the volume-averaged pressure and $\langle\rho\rangle$ is the volume-averaged energy density. (We can also use these quantities as a check of the numerical simulation, since $\frac{d}{dt}(V\langle\rho\rangle) = \langle p\rangle\frac{dV}{dt}$.) We examine the change in the average equation of state as inflation nears its end, where w increases from the vacuum-dominated value $w = -1$ to positive values as reheating produces radiation, to finally approach the matter-dominated value $w = 0$, as the inflaton performs small oscillations about the minimum at $\phi = \nu$. In the latter phase, both oscillons and perturbative waves behave as pressureless dust. Results are shown in Fig. 3 for different values of the coupling h, from weak ($h = \sqrt{\lambda}/100$, left) to strong ($h = \sqrt{\lambda}$, right). In Fig. 4 we plot the equation of state for $h = 0$, that is, with no coupling between the two fields.

As above, in Figs. 3 and 4 the vertical dashed line (red online) marks the time when oscillations of the inflaton can no longer climb above the inflection point. First we note that when the two fields are coupled ($h \neq 0$), the overall behavior of the equation of state is quite insensitive to the coupling strength h. This is consistent with the results of Fig. 1, where no noticeable difference was seen for the evolution of ϕ for different values of h. We also note that, in all cases, there is a sharp change in the equation of state as the pressure becomes positive definite. (There are a few oscillations back to negative pressure, but these are small-amplitude and would disappear upon time-averaging.) There is, however, a clear difference between the coupled and uncoupled cases. While for $h = 0$ the transition to positive-definite pressure happens *at the time* when ϕ drops beyond the inflection point, $\phi \geq \phi_{\rm inf}$ (cf. Fig. 4), for $h \neq 0$ the discontinuity happens before $\phi > \phi_{\rm inf}$ (cf. Fig. 3). Again, this is consistent with the general behavior shown

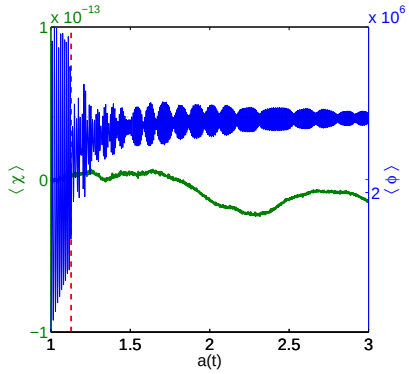

FIG. 2: (Color online.) Volume-averaged values of ϕ and χ as functions of the expansion factor $a(t)$, in units of m_ϕ, for the decoupled case. Results are shown for $\lambda = 1.5 \times 10^{-13}$, $m_{\rm pl} = 100\nu$, and $h = 0$. The vertical dashed line indicates the time when oscillations of the inflaton can no longer reach the inflection point.

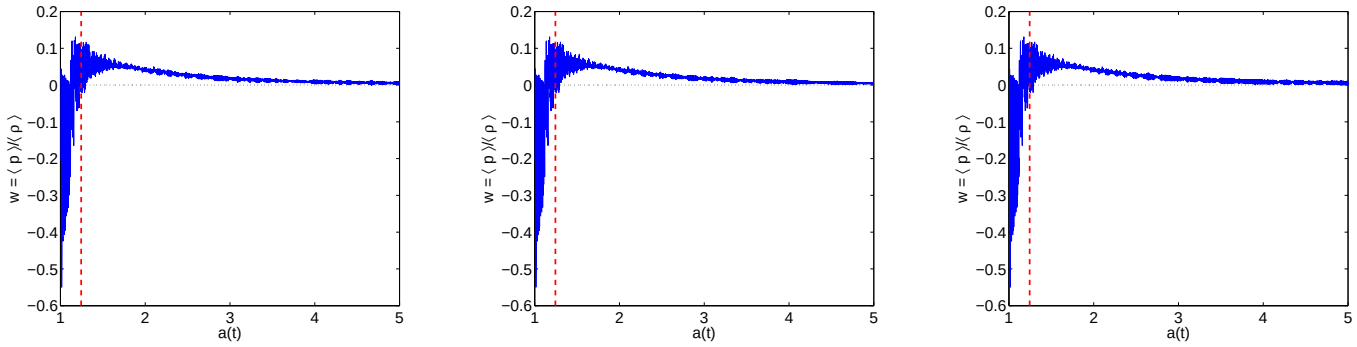

FIG. 3: (Color online.) Equation of state $w = \langle p \rangle / \langle \rho \rangle$ as a function of the expansion factor $a(t)$, averaged in time over one oscillation period of the inflaton field. The calculation is shown for $\lambda = 1.5 \times 10^{-13}$, $m_{\rm pl} = 100\nu$, and $h = \sqrt{\lambda}/100$ (left), $h = \sqrt{\lambda}/10$ (center), and $h = \sqrt{\lambda}$ (right). The vertical dashed line denotes the time when oscillations of the inflaton drop below the inflection point.

in Fig. 1, where the coupling between the two fields sustains transient nonlinear oscillations of the inflaton beyond the inflection point.

As we will see next, the sharp change in behavior of the equation of state marks the beginning of oscillon formation for all values of h we investigated. Also, the peak oscillon formation happens just before and around where $\phi \lesssim \phi_{\rm inf}$. This is the maximum of the relative configurational entropy (RCE), which reliably detects the presence of spatially-extended objects in the simulation volume. Before we can show our results for oscillons, we briefly review the RCE.

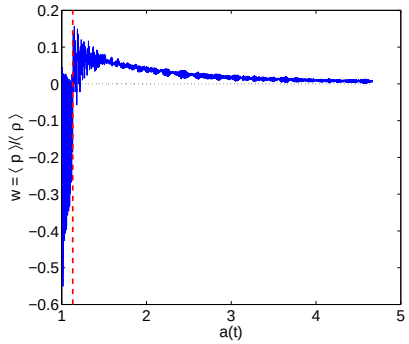

FIG. 4: (Color online.) Equation of state $w = \langle p \rangle / \langle \rho \rangle$ as a function of the expansion factor $a(t)$, averaged in time over one oscillation period of the inflaton field, for the decoupled case. The calculation is shown for $\lambda = 1.5 \times 10^{-13}$, $m_{\rm pl} = 100\nu$, and $h = 0$. Note the sharp change in the equation of state at the time when $\phi \geq \phi_{\rm inf}$ denoted by the dashed vertical line.

B. Relative Configurational Entropy

We use two measures to quantify the formation of oscillons. First, as a heuristic estimate, we calculate the fraction of the system's total energy that is located in regions where the energy density is more than six times the average energy density of the system. This quantity is initially negligible, and would remain constant under linear de Sitter expansion. Second, we use the relative configurational entropy (RCE) for the energy density [38], which provides an efficient quantitative measure for the presence of coherent classical field configurations in general nonlinear models [37]. (We have verified that both measures remain trivial for a particle rolling down an ordinary ϕ^4 potential without spontaneous symmetry breaking, in which case no oscillons form.) As proposed in Ref. [38], the RCE is the field-theory equivalent of the Kullback-Leibler divergence of information theory, used there to discriminate between an arbitrary bit string and a fixed baseline or reference string [40], giving a probabilistic measure of the expected number of extra bits required to code samples of the desired string in terms of the baseline. In other words, the Kullback-Leibler divergence offers a "distance" in information complexity between the two strings. (It is not a true metric, however, since it is not symmetric in its arguments.) In field theory, the RCE will give a "distance" in Fourier field configuration space between the measured fields and the baseline. In particular, following [38], we define the RCE in terms of a modal fraction $f(\boldsymbol{k}, t)$ computed from the energy density $\rho(\boldsymbol{x}, t)$,

$$f(\boldsymbol{k}, t) = \frac{|\rho(\boldsymbol{k}, t)|^2}{\int |\rho(\boldsymbol{k}, t)|^2 d^3\boldsymbol{k}}, \tag{9}$$

where $\rho(\boldsymbol{k}, t)$ is the spatial Fourier transform of the energy density. For the baseline $g(\boldsymbol{k})$, we use the modal fraction computed from our initial conditions — a system of quantum oscillators — in which each mode carries an average energy $\omega/2$. We then write the RCE as

$$S_f(t) = \int d^3\boldsymbol{k} f(\boldsymbol{k}, t) \ln \frac{f(\boldsymbol{k}, t)}{g(\boldsymbol{k})} \,. \tag{10}$$

The RCE provides a measure for the departure of our system from featureless quantum initial conditions. As shown in Ref. [38], the RCE is extremely accurate when used to identify coherent configurations in nonlinear field models, showing a linear scaling with the number density of objects present. In Ref. [38], finite temperature spontaneous symmetry breaking in a simple double-well model was investigated, and the baseline was thus a purely thermal spectrum. Here, we use the RCE to identify the presence of coherent objects in an expanding cosmological background. The more pronounced the departure between the signal $f(\boldsymbol{k}, t)$ and the baseline $g(\boldsymbol{k})$, the larger the RCE. As described in Ref. [38], a larger RCE is equivalent to a higher density of coherent field configurations in the system.

C. Oscillon Formation

In Fig. 5 we show the results from our two measures for the emergence of oscillons: one based on an excess of energy density over the average density of the system, and the other based on the RCE. Results are shown for $h \neq 0$ as functions of the scale factor $a(t)$. For contrast, in Fig. 6 we show the same quantities for $h = 0$, where oscillons are also present. We see that oscillons initially contribute some 30% of the energy density in all cases, falling down to about 3% for late times when $h \neq 0$ and to about 6% for $h = 0$.

The oscillons we see consist of localized oscillations of the ϕ field. As an illustration, Fig. 7 shows a 2d slice of the energy density at the end of each simulation, with oscillons clearly distinguished from the much smaller energy density associated with perturbative waves.

Differences between the three plots in Fig. 5 are noticeable only for times $a(t) \gtrsim 2.2$, as expected from the bottom row of Fig. 1. As in other preheating particle-production studies [30, 31, 41], oscillons form as nonlinear effects fed by parametric resonance due to oscillations of the inflaton become dominant. In our case, this is marked by a sharp change in the behavior of the inflaton, already apparent in Fig. 1: notice a drop in oscillation amplitude for all three cases around $a(t) \sim 1.12$. To see this more clearly, in Fig. 8 we show the evolution of the inflaton and the oscillon count for early times for both $h \neq 0$ and $h = 0$. The evolution is the same for all values of h until about $a(t) \sim 1.12$, which is when the effects from the χ field become relevant (that is, when its amplitude raises sufficiently above zero to influence the dynamics of the inflaton), in particular by keeping the oscillation amplitude of the inflaton larger for a longer period of time.

The change in the dynamics of the inflaton is clearly reflected in the equation of state, as can be seen in Fig. 3 and, in detail, in Fig. 9. For $h \neq 0$, this transition happens when ϕ undergoes a drop in oscillation amplitude, but still before it drops beyond its inflection point at the vertical dashed line. This change in the equation of state marks the

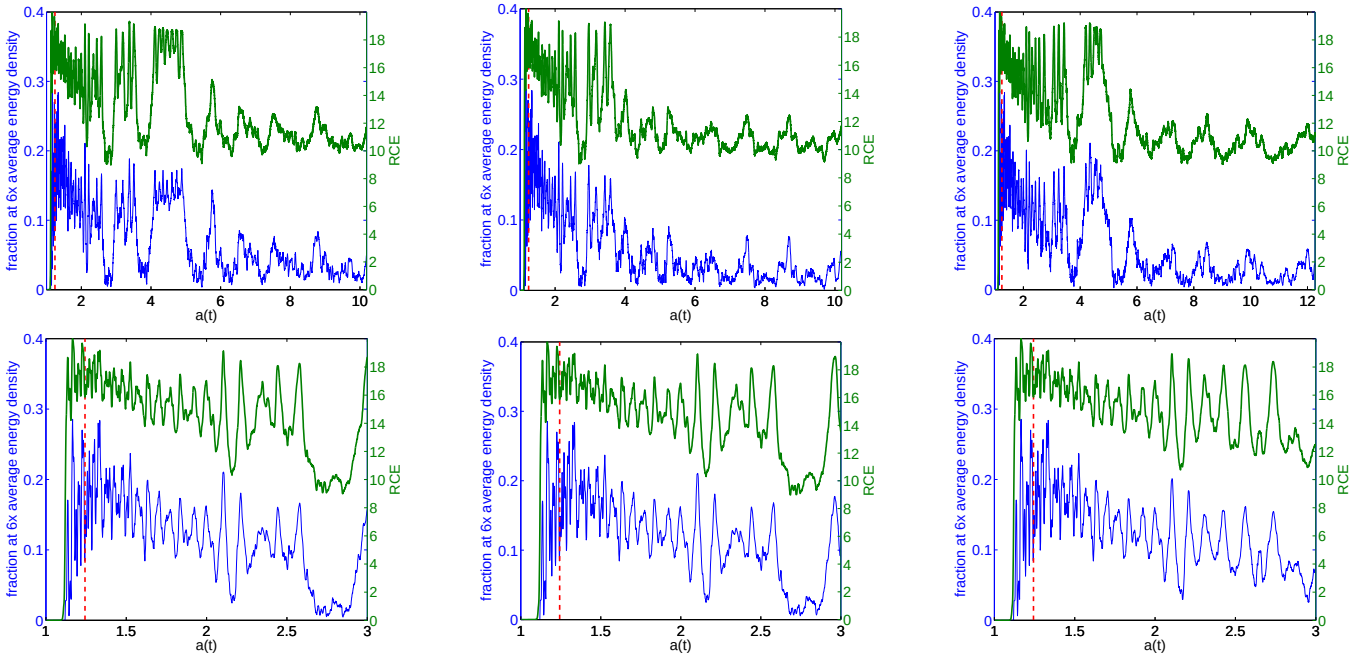

FIG. 5: (Color online.) Oscillon formation as a function of the expansion factor $a(t)$, as measured by the fraction of the system's total energy located in regions where the energy density is more than six times the average energy density (dashed line) and by the relative configurational entropy (continuous line). Both have been averaged in time over approximately one oscillation period of the inflaton field. The calculation is shown for $\lambda = 1.5 \times 10^{-13}$, $m_{\rm pl} = 100\nu$, and $h = \sqrt{\lambda}/100$ (left), $h = \sqrt{\lambda}/10$ (center), and $h = \sqrt{\lambda}$ (right). The vertical line denotes the time when $\phi > \phi_{\rm inf}$. The bottom row shows the details of the evolution for shorter times.

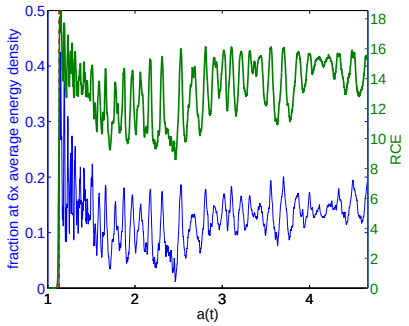

FIG. 6: (Color online.) Oscillon formation as a function of the expansion factor $a(t)$, as measured by the fraction of the system's total energy located in regions where the energy density is more than six times the average energy density (dashed line) and by the relative configurational entropy (continuous line), for the decoupled case. Both have been averaged in time over approximately one oscillation period of the inflaton field. The calculation is shown for $\lambda = 1.5 \times 10^{-13}$, $m_{\rm pl} = 100\nu$, and $h = 0$. The vertical line denotes the time when $\phi > \phi_{\rm inf}$.

onset of oscillon formation. For $h = 0$, the drop in oscillation amplitude of the inflaton coincides with its drop below the inflection point. There is a sharp transition at this point in the number of oscillons formed. This clear correlation between the change in the behavior of the inflaton, the sign change in the equation of state, and the onset of oscillon formation justifies our characterization of oscillon formation as a transition to order during preheating.

The fraction of energy we measure in oscillons shows long-term oscillations as the configurations undergo "breathing" over long times [20]. We expect this variation to gradually die out, leaving on average about 3% of the total energy of the universe in oscillons, a result that appears to be independent of the coupling h to the light field.

The RCE shows analogous results, as can be seen directly in Figs. 5 and 6. It has less variability, since it does not involve the arbitrary cutoff at six times the average energy density. Our results demonstrate that the RCE is a reliable measure of the emergence of localized order in field theories, even with an expanding background. Since the value of the RCE correlates directly with the number of localized coherent states (see Ref. [38]), it can be used as a

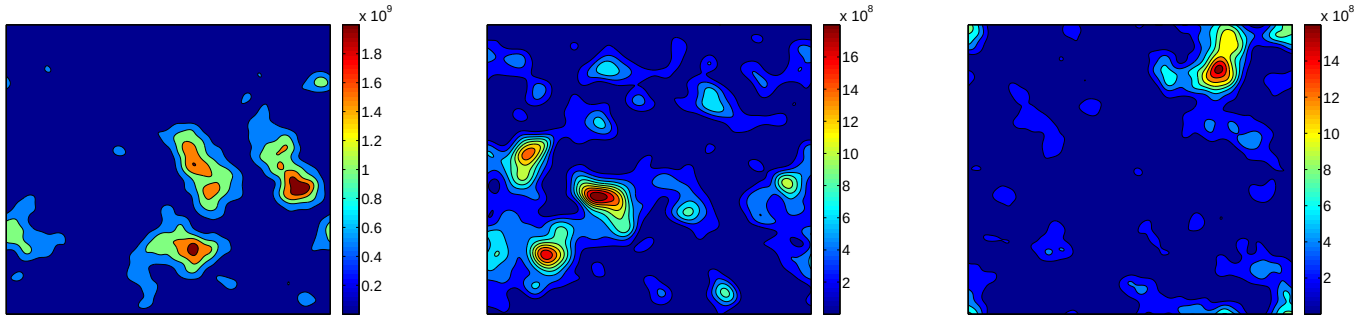

FIG. 7: (Color online.) A 2d slice of the energy density in units of m_ϕ^4 at the end of the simulation for $\lambda = 1.5 \times 10^{-13}$, $m_{\rm pl} = 100\nu$, and $h = \sqrt{\lambda}/100$ (left), $h = \sqrt{\lambda}/10$ (center), and $h = \sqrt{\lambda}$ (right). Oscillons are clearly visible, standing far above the contribution from perturbative waves.

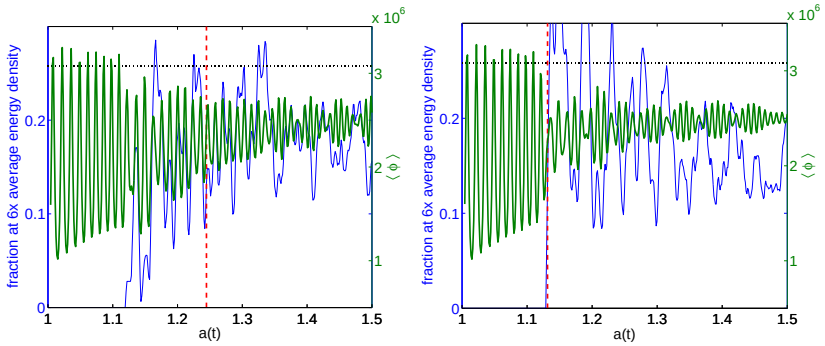

FIG. 8: (Color online.) Early time evolution of the volume-averaged inflaton (continuous line) and oscillon count (dashed line) for $h = \sqrt{\lambda}/100$ (left) and $h = 0$ (right). (Results for other two cases with $h \neq 0$ are essentially the same for these short times.) The vertical line denotes the time after which $\phi > \phi_{\rm inf}$. Oscillon formation starts when there is a marked drop in the oscillation amplitude of the inflaton. Notice that for $h \neq 0$ this happens *before* the inflaton falls beyond the inflection point (at $a(t) \sim 1.25$), while for $h = 0$ the two events coincide.

measure of complexity, that is, of the presence of ordered structures emerging from a disordered background.

From both measures it is clear that oscillons form in significant quantities during preheating and a fraction of them remain stable over cosmological time-scales. Indeed, we see no indication that they decay during our simulations. As a result, oscillons can play an important role during reheating, as the universe transitions to a power-law, radiation-dominated, and then matter-dominated expansion. At least for models where oscillons form — and they appear to be quite general — any analysis of reheating that neglects their presence would clearly be incomplete.

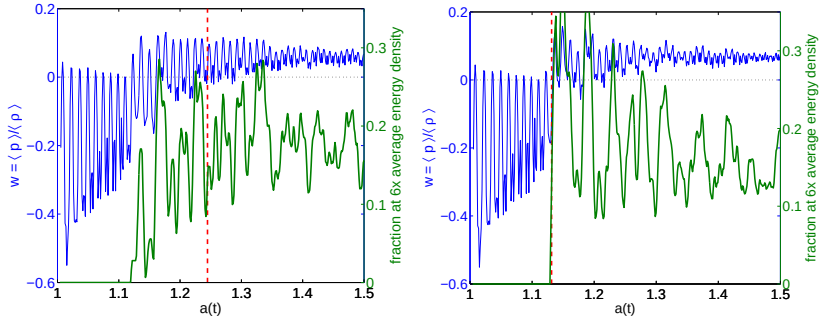

FIG. 9: (Color online.) Early time evolution of the equation of state (dashed line) and oscillon count (continuous line) for $h = \sqrt{\lambda}/100$ (left) and $h = 0$ (right). (Results for other two cases with $h \neq 0$ are essentially the same for these short times.) For all values of h, oscillon formation begins when the equation of state becomes positive, which is when the inflaton oscillations undergo a clear drop in amplitude, as can be seen from Fig. 8.

IV. SUMMARY AND OUTLOOK

We investigated the preheating dynamics of a hilltop model of inflation where the inflaton field is coupled quadratically to a massless scalar field. Our goals where threefold: first, to search for the emergence of localized nonperturbative structures during preheating; second, to investigate the effect of the massless field on the emergence and stability (longevity) of these structures; third, to test the use of the relative configurational entropy as a measure of the emergence of ordered structures in a cosmological setting.

In order to achieve our goals we solved the coupled Friedmann-Klein-Gordon equations in a expanding spacetime. Starting from quantum initial conditions with the inflaton partway down its slow roll toward the potential minimum, we used a parallel code to extend our runs for very long cosmological times, of order $15,000 m_\phi^{-1}$. We chose couplings consistent with the combined Planck+WMAP+BAO data.

We found that ordered structures in the form of oscillons emerged for $0 \leq h/\sqrt{\lambda} \leq 1$ and that these structures persisted for the duration of our runs contributing roughly 3% of the total energy density. Most interestingly, we found that the production of ordered structures has a clear signature as a transition in the effective equation of state and in the behavior of the volumed-averaged inflaton: for all values of the coupling between the two fields, oscillons start to form as the oscillation amplitude of the inflaton undergoes a clear drop. The transition into oscillon nucleation can be clearly identified in the equation of state, which turns positive as the first structures appear. In the absence of coupling between the two fields ($h = 0$), the change in the equation of state is quite abrupt, happening when the inflaton rolls beyond its inflection point [See Fig. 9 (right)]. When $h \neq 0$, the nonlinear coupling between the two fields sustains larger-amplitude oscillations for the inflaton, so that by the time it drops beyond the inflection point oscillon formation is well underway [See Fig. 9 (left)]. We established that the relative configurational entropy gives a clear reading of the emergence of ordered structures, with the added bonus of being independent of an arbitrary scale in the energy density.

Our results, taken together with other studies listed in the references, (see, e.g., Refs. [11, 23, 24, 28–32]) indicate that the emergence of ordered structures is a very general feature of preheating for potentials that support them. Their presence delays thermodynamic equipartition since they "lock" long wavelength modes for a long time. The fact that oscillons persist for cosmologically long time-scales shows that thermodynamic equilibrium is never quite reached, or is delayed for as long as such structures remain present. Studies of reheating and the reheating temperature of the universe must consider this situation in detail. Could there have been an epoch of strong entropy generation due to the decay of such structures? More generally, if we adopt the view that the Big Bang is really the reheating of the universe after inflation, it seems that the universe starts not only with an explosive production of particles but also with a vibrant population of time-dependent oscillon-like structures.

Acknowledgments

MG was supported in part by a National Science Foundation grant PHY-1068027 and by a Department of Energy grant de-sc0010386. MG also acknowledges support from the John Templeton Foundation grant under the New Frontiers in Astronomy & Cosmology program. NG was supported in part by NSF grant PHY-1213456.

[1] Planck Collaboration: P. A. R. Ade *et al.*, *Planck 2013 results XXII. Constraints on Inflation*, arXiv:1303.5082. Submitted to Astronomy and Astrophysics.
[2] Planck Collaboration: P. A. R. Ade *et al.*, *Planck 2013 results I. Overview of Products and Scientific Results*, arXiv:1303.5062. Submitted to Astronomy and Astrophysics.
[3] A. Ijjas, P. J. Steinhardt, and A. Loeb, Phys. Lett. B **723**, 261 (2013).
[4] C. L. Bennett et al., Ap. J. S **208**, 20B (2013).
[5] For a reiew, see, D. Weinberg et al., in press Phys. Rept. [arXiv:1201.2434v2].
[6] A. Albrecht and P. J. Steinhardt, Phys. Rev. Lett. **48**, 1220 (1982).
[7] A. D. Linde, Phys. Lett. B **108**, 389 (1982).
[8] S. Dodelson, W. H. Kinney, and E. W. Kolb, Phys. Rev D **56**, 3207 (1997).
[9] A. R. Liddle and D. H. Lyth, Phys. Rept. **231**, 1 (1993).
[10] B. A. Bassett, S. Tsujikawa and D. Wands, Rev. Mod. Phys. **78**, 537 (2006).
[11] G. N. Felder, L. Kofman, and A. D. Linde, Phys. Rev D **64**, 123517 (2001); D. Podolsky, G. N. Felder, L. Kofman, and M. Peloso, Phys. Rev. D **73**, 023501 (2006).
[12] D. Boyanovsky et al., Phys. Rev. D **56**, 1939 (1997).
[13] K. Freese, J. A, Frieman, and A. V. Olinto, Phys. Rev. Lett. **65**, 3233 (1990).

[14] F. C Adams et al., Phys. Rev. D **47**, 426 (1993).
[15] I. L. Bogolubsky and V. G. Makhankov, JETP Lett. 24 (1976) 12 [Pis'ma Zh. Eksp. Teor. Fiz. 24 (1976) 15].
[16] M. Gleiser, Phys. Rev. **D49**, 2978 (1994).
[17] E. J. Copeland, M. Gleiser, and H. R. Muller, Phys. Rev. **D52**, 1920 (1995), hep-ph/9503217.
[18] M. Gleiser and J. Thorarinson, Phys. Rev. D **76**, 041701(R) (2007); *ibid.*, **79**, 025016 (2009).
[19] V. Achilleos, F.K. Diakonos, D.J. Frantzeskakis, G.C. Katsimiga, X. N. Maintas, E. Manousakis, C.E. Tsagkarakis, and A. Tsapalis, Phys. Rev. D **88** 045015 (2013).
[20] E. Farhi, N. Graham, V. Khemani, R. Markov and R. Rosales, Phys. Rev. D **72**, 101701 (2005).
[21] N. Graham, Phys. Rev. Lett. **98**, 101801 (2007); [Erratum-ibid. **98**, 189904 (2007)]; N. Graham, Phys. Rev. D **76**, 085017 (2007).
[22] E. I. Sfakianakis, [arXiv:1006.3075].
[23] E. J. Copeland, S. Pasoli and A. Rajantie, Phys. Rev. D **65**, 103517 (2002).
[24] J. McDonald, Phys. Rev. D **66**, 043525 (2002); M. Broadhead and J. McDonald, Phys. Rev. D **72**, 043519 (2005).
[25] N. Graham and N. Stamatopoulos, Phys. Lett. B **639**, 541 (2006).
[26] E. Farhi, N. Graham, A. Guth, N. Iqbal, R. Rosales and N. Stamatopoulos, Phys. Rev. D **77**, 085019 (2008).
[27] M. A. Amin, [arXiv:1006.3075]; M. A. Amin, R. Easther and H. Finkel, JCAP, 1012:001 (2010)
[28] M. A. Amin and D. Shirokoff, Phys. Rev. D **81** 085045 (2010).
[29] M. Gleiser, N. Graham, and N. Stamatopoulos, Phys. Rev. D **82**, 043517 (2010).
[30] M. Gleiser, N. Graham, and N. Stamatopoulos, Phys. Rev. D **83**, 096010 (2011).
[31] M. A. Amin, R. Easther, and H. Finkel, JCAP **21**, 001 (2010)
[32] M. A. Amin, R. Easther, H. Finkel, R. Flauger, and M. P. Hertzberg, Phys. Rev. Lett. **108**, 241302 (2012).
[33] M. P. Hertzberg, Phys. Rev. D **82**, 045022 (2010).
[34] M. Gleiser, Int. J. Mod. Phys. D **16**, 219 (2007).
[35] M. Gleiser and A. Heckler, Phys. Rev. Lett. **76**, 180 (1996).
[36] S.-Y. Zhou, E. J. Copeland, R. Easther, H. Finkel, Z.-G. Mou, and P. M. Saffin, in press, JHEP [arXiv:1304.6094].
[37] M. Gleiser and N. Stamatopoulos, Phys. Lett. B **713**, 304 (2012).
[38] M. Gleiser and N. Stamatopoulos, Phys. Rev. D **86** 045004 (2012).
[39] S. Weinberg, *Gravitation and Cosmology: Principles and Applications of the General Theory of Relativity* (J. Wiley & Sons, New York, 1972).
[40] S. Kullback and R. A. Leibler, Ann. Math. Stat. **22**, 79, (1951).
[41] G. Felder, J. Garcia-Bellido, P. B. Greene, L. Kofman, A. D. Linde and I. Tkachev, Phys. Rev. Lett **87**, 011601 (2001).